Corrosion Kinetics of Stainless Steel by Hydrogen Measurement under Deep Geological Repository Condition - 16047

Tomofumi Sakuragi 1*, Satoshi Yoshida 1*, Junichiro Kinugasa 2**, Osamu Kato 2**, and Tsuyoshi Tateishi 3***
* Radioactive Waste Management Funding and Research Center, 1-15-7 Tsukishima, Chuo City, Tokyo 104-0052, Japan,
** Kobe Steel, Ltd., 2-2-4, Wakinohama-Kaigandori, Chuo Ward, Kobe 651-8585, Japan,
*** Kobelco Research Institute, Inc., 1-5-5 Takatsukadai, Nishi Ward, Kobe 657-2271, Japan

ABSTRACT

Spent fuel assemblies consisting of stainless steels are expected to be disposed of in a deep underground repository. The radionuclides release and gas generation from activated metallic wastes in a disposal system will be controlled by the corrosion reaction. Most studies on stainless steel corrosion have been investigated under corrosion rates around several $\mu m \cdot a^{-1}$. A recent study has revealed that the corrosion rate of stainless steel is extremely slow—less than $nm \cdot a^{-1}$ at 303 K. In the present study, corrosion kinetics at different temperatures up to 353 K were evaluated from the oxidation reaction by hydrogen gas measurement using 18Cr−8Ni austenitic stainless steel in a deoxygenated glass ampoule filled with a dilute NaOH solution of pH 12.5 for 24 months. Uniform corrosion and a reaction of $3Fe + 4H_2O \rightarrow Fe_3O_4 + 4H_2$ were assumed. After 24 months, the corrosion rates, which decreased with time but increased with rising temperature, were on average 7.80×10^{-4}, 2.65×10^{-3}, and 7.62×10^{-3} $\mu m \cdot a^{-1}$ at 303 K, 323 K, and 353 K, respectively. The corrosion kinetics were found to follow a parabolic rate law, which suggests the corrosion process is under diffusion control. The activation energy evaluated by the Arrhenius relationship of the parabolic rate constants has been determined to be 82.5 ± 6.2 kJ/mol, which corresponds to the values at high temperatures down to 423 K.

INTRODUCTION

Management and safe disposal of activated metal wastes are challenges for advancing nuclear fuel reprocessing and decommissioning of nuclear power plants. The wreckage of spent fuel assemblies consist of stainless steels that are mixed and compressed, and then the compacts are stuffed into stainless steel canisters. These canisters are expected to be disposed of in a deep underground repository as Group 2 category of TRU waste in Japan [1]. Carbon 14 (C-14) is a typical activated product in metals and is mainly generated by the $^{14}N(n,p)^{14}C$ reaction. Stainless steel nozzles account for 16% of the weight of the hull and endpiece waste, and their C-14 corresponds to 28% of the total C-14 inventory [2]. The radionuclide release and gas generation from the metallic wastes in a disposal system is controlled by a corrosion reaction together with the simultaneous cathodic reaction of water reduction.

Regarding stainless steel corrosion under alkaline condition, numerous studies have focused on reinforce behavior in concrete or on durability under caustic environments. Most of these studies were investigated under oxygenated conditions and concerned with a corrosion rate around several $\mu m \cdot a^{-1}$. The corrosion behavior of stainless steels under these anticorrosive repository conditions (low oxygen, high alkaline, and in situ temperature under 353 K) has been consequently outstanding, in large part because the corrosion rate is too small to be clearly comprehended by common methods [3]. The basis for the metal corrosion rate as a safety assessment parameter in Japan, where the maximum temperature permitted at the waste form interface is 353 K, comes from the results of limited experimentation performed at 308 K in the presence of 3,200 ppm chloride [1]. A recent study by the authors has revealed the overconservativeness of basing the stainless steel corrosion rate on long-term hydrogen measurements at 303 K [4]. This corrosion rate is less than $nm \cdot a^{-1}$, which is 50 times slower than the rate assumed in the Japanese safety assessment.

To achieve a better understanding of the corrosion behavior that occurs over long disposal times, concerns such as investigating the kinetics in detail must be addressed. Aqueous corrosion of stainless steels is generally described by a model in which the formation of passive Cr oxide limits the transport of Fe ions. Robertson [5] published parabolic corrosion rate constants at high temperatures down to 423 K and presented a high-temperature corrosion model of stainless steels from the point of view of oxide characterizations based on several studies involving measurement of electrochemical and weight changes [6]. In our previous study performed at 303 K, the time dependence of the corrosion has also exhibited the behavior of a parabolic rate law during a one year period from the start of test [4].

The purpose of the present study is to evaluate the corrosion kinetics of austenitic stainless steel at various in situ temperatures up to 353 K. High pH and deoxygenated conditions were selected to simulate the typical underground repository environment. Batch tests using a glass ampoule were performed over two years, during which the amounts of gaseous hydrogen that evolved from the corrosion reaction ($3Fe + 4H_2O \rightarrow Fe_3O_4 + 4H_2$) were measured. The parabolic rate constant of the corrosion was obtained by following the method described in previous studies [5]. The corrosion process is then discussed with activation energy and oxide characteristics.

EXPERIMENTAL

The 18Cr−8Ni austenitic stainless steel with a thickness of 0.1 mm was obtained from Nilaco Corporation (Product No. 753323). The inspection data for the chemical composition is shown in Table I. The stainless steel sheet was polished with 0.02 mm alumina powder and then cut. The average diameter of the grains was approximately 15 μm, and the initial oxide thickness was approximately 3 nm. The detailed properties for the specimen are described in a separate study [4].

Table I. Composition of stainless steel used in corrosion tests (in wt%, from inspection data). Values in parenthesis represent the specification (Japanese Industrial Standard G 4305).

C	Si	Mn	P	S	Ni	Cr
0.07 (< 0.08)	0.45 (< 1.00)	0.79 (< 2.00)	0.028 (< 0.045)	0.005 (< 0.030)	8.29 (8.00-10.50)	18.14 (18.00-20.00)

An ampoule batch experiment described by Mihara et al. [7] and Honda et al. [8] was applied (Fig. 1). The stainless steel strips (22 pieces; 3 mm×90 mm×0.1 mm, surface area of 1.19×10^{-2} m^2) were set in glass ampoules. A stop-cock was attached, then the ampoule was filled with an NaOH solution (pH 12.5) and the stop-cock closed. This enclosure procedure was performed in a glove box that had been purged by nitrogen gas with oxygen concentration below 0.1 ppm. The ampoules were moved outside the glove box and sealed by heating. At appropriate corrosion times up to 24 months under controlled temperatures, the ampoules were set on a vacuum gas collection system that connected to gas chromatography equipment (YANACO G-2800) and the hydrogen gas was measured.

Surface oxide characteristics were examined after corrosion. The cross section of the oxide layer was observed by TEM (JEOL, JEM-2010F) and analyzed by EDX (NORAN Instruments, Vantage EDX) for a sample prepared by using FIB (Hitachi, FB2000A) after the vacuum deposition of carbon. The elemental distribution of the surface was measured by XPS (Physical Electronics, Quantera SXM).

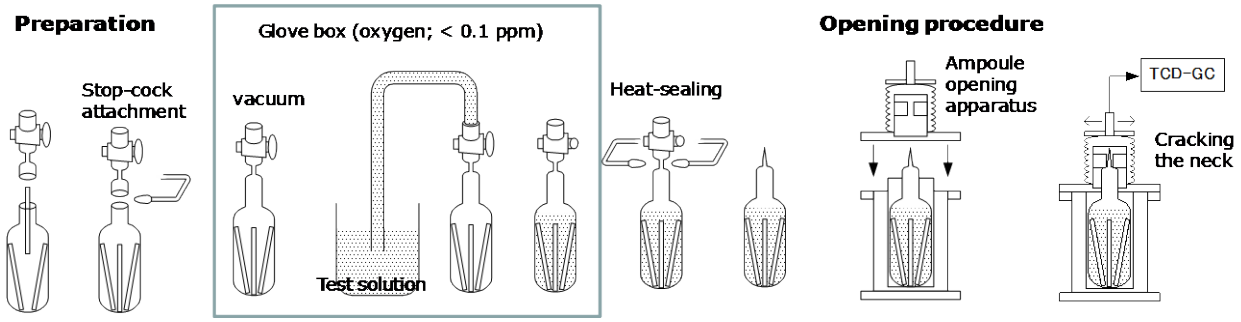

Fig. 1. Overview of the glass ampoule corrosion setup [7, 8].

RESULTS AND DISCUSSION

In order to evaluate the corrosion rate of the stainless steel from the evolved hydrogen, the following corrosion reaction is assumed based on previous studies [1, 4].

$$3Fe + 4H_2O \rightarrow Fe_3O_4 + 4H_2. \qquad \text{(Eq. 1)}$$

Because hydrogen absorption into the stainless steel is negligible (less than 3% in our previous study [4]), it is acceptable to count only the gaseous hydrogen for evaluating the stainless steel corrosion in this system. The corrosion rate R_c ($\mu m \cdot a^{-1}$), which represents the amount of iron consumed by oxidation under

stoichiometry in the above reaction and is assumed to be a uniform rate, can therefore be obtained from the following reaction.

$$R_c = \frac{3}{8} \cdot \frac{A_{gas} \cdot M_{Fe} \cdot 10^6}{\rho_{Fe} \cdot t} \qquad \text{(Eq. 2)},$$

where A_{gas} is the atomic molar amount of hydrogen gas per unit surface area ($mol \cdot m^{-2}$), M_{Fe} is the molecular weight of iron (55.85 $g \cdot mol^{-1}$), ρ_{Fe} is the iron density (7.87×10^6 $g \cdot m^{-3}$), and t is the test time.

Fig. 2 shows the results of R_c as a function of time at different temperatures. The figure also includes two sets of our previous data (dashed lines) obtained by a gas flow system that monitored the hydrogen gas continuously [4]. As stated above, these corrosion rates are considered to be uniform. The values of R_c decreased as the corrosion period increased and as temperature decreased. After 24 months, the average R_c values of the two data sets were 7.80×10^{-4} at 303 K, 2.65×10^{-3} at 323K, and 7.62×10^{-3} $\mu m \cdot a^{-1}$ at 353 K. To avoid degradation of the filling cementitious material, the criterion for permissible temperature in the Japanese disposal concept is 353 K at the waste form interface [1]. By this criterion, it is consequently confirmed that the R_c value of 2.0×10^{-2} $\mu m \cdot a^{-1}$, the estimated value for stainless steel corrosion in the safety assessment in Japan (TRU-2 report) [1], is sufficiently conservative.

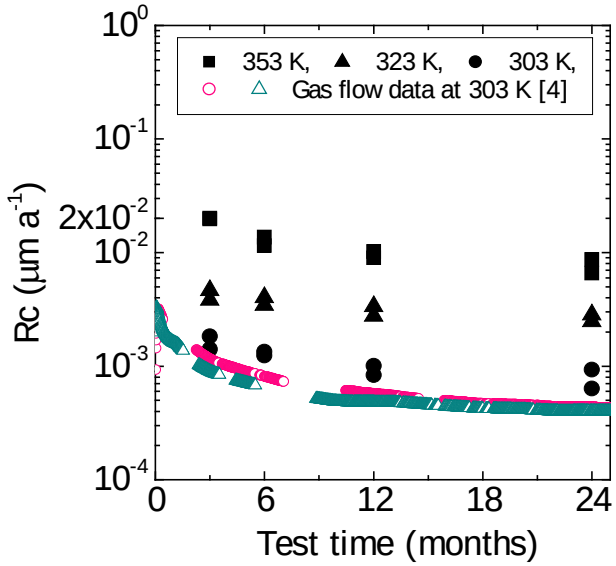

Fig. 2. Corrosion rate of stainless steel (R_c) at different temperatures. The continuous data are obtained by a gas flow system [4].

The present data from ampoule tests at 303 K show slightly larger corrosion rates than previous data obtained by a gas flow system [4]. This difference in results according to the experimental method was also observed for the corrosion of zirconium alloys [9]. Unpolished metals show a trend of rapid corrosion. This result may be attributable to the fact that the surface area of the unpolished edge was a

larger ratio of the specimen area for the batch ampoule test than for the gas flow test [9].

Considering the long-term behavior of stainless steel corrosion after disposal, it is important to understand and model the corrosion mechanism. The kinetic behavior of aqueous corrosion of stainless steel has been discussed by Robertson for high temperatures down to 423 K together with a summary of parabolic corrosion rate constants, k_p ($cm^2 \cdot sec^{-1}$) from the following equation [5].

$$x^2 = k_p \cdot t \qquad \text{(Eq. 3)},$$

where x is the thickness (in cm) of magnetite, Fe_3O_4, and t is the test time (in sec.). Note that the x value used by Robertson was the total thickness of metal loss originally obtained by Maekawa et al. using A304 austenitic stainless steels in neutral, de-aerated, and stationary water in the temperature range from 423 K to 633 K [6]. Our previous corrosion study, in which hydrogen generation was monitored continuously at 303 K, has shown that the stainless steel corrosion has a good parabolic relationship with time up to one year [4]. This result enables the parabolic rate constant (k_p) for in situ temperatures to be evaluated. In the present study, the thickness of magnetite x can be calculated by the following equation, based on Eq. 1.

$$x = \frac{1}{8} \cdot \frac{M_{Fe3O4} \cdot A_{gas}}{\rho_{Fe3O4}} \cdot 100 . \qquad \text{(Eq. 4)},$$

where M_{Fe3O4} and ρ_{Fe3O4} are the molecular weight (231.55 $g \cdot mol^{-1}$) and density (5.2×10^6 $g \cdot m^{-3}$) of magnetite. Fig. 3 summarizes the relationship between x and time according to Eq. 3. The corrosion kinetics exhibit a parabolic rate relationship fairly well.

Fig. 4 shows the Arrhenius relationship of the parabolic rate constant (k_p) of stainless steel corrosion together with the high temperature data down to 423 K [6]. The k_p values in the present study are larger than those extrapolated from the data by Maekawa et al. and slightly larger than those obtained by the gas flow system described above [4]. The activation energy has been determined and found to be 82.5 ± 6.2 kJ/mol, which corresponds to the value of 74.4 ± 6.0 kJ/mol that is shown under high temperatures down to 423 K. This result suggests that the basic corrosion mechanism is similar at both high and in situ temperatures. At high temperature, the kinetic behavior of aqueous corrosion of stainless steel has been discussed by Robertson [6], who explained that the formation of duplex oxide on a metal surface and the diffusion of Fe ions through the oxide are considered to be rate controlling for the corrosion. The oxide characteristics formed under in situ temperature are discussed below. The corrosion data are summarized in Table II.

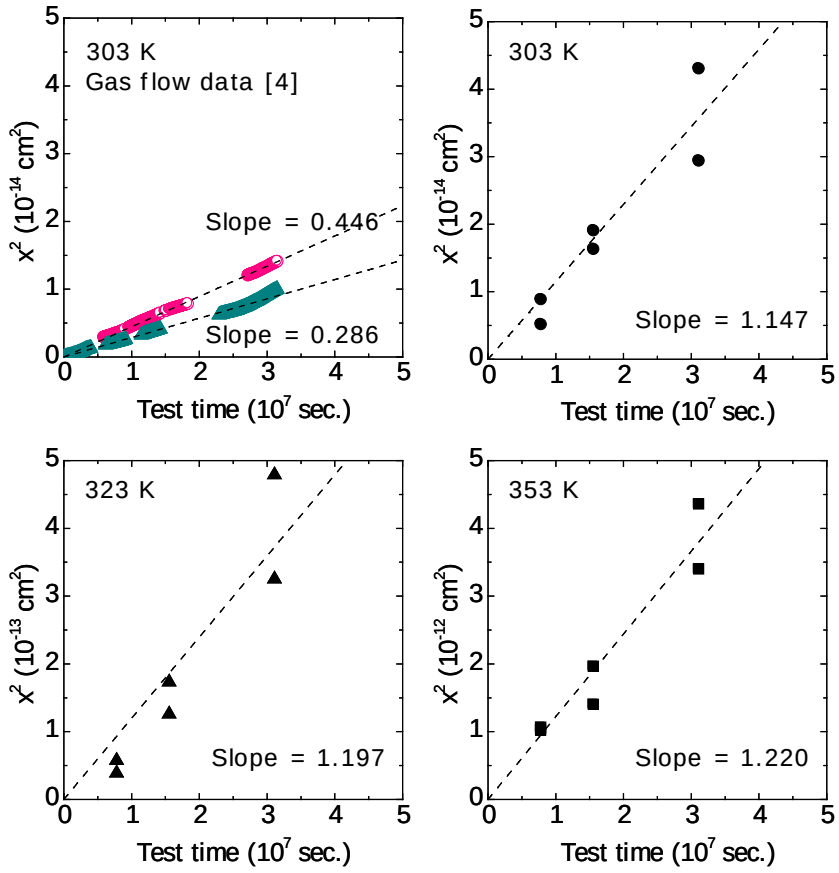

Fig. 3. The relationship between square root of oxide thickness and test time in Eq 3. Lines come from linear regressions.

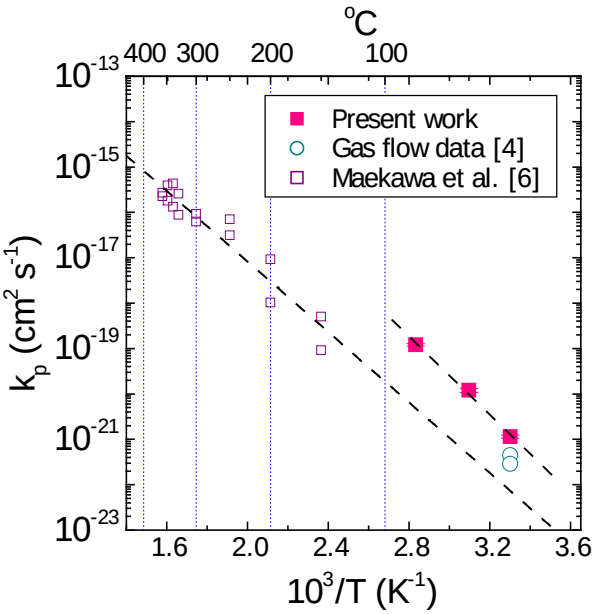

Fig. 4. The parabolic rate constants of stainless steel corrosion. Dashed lines are least square fits.

The surface oxide formed after corrosion was analyzed by TEM coupled with EDX and electron diffraction. Fig. 5 shows the cross section of the oxide layer observed by TEM. There are three parts depicted in the image—metal, oxide film, and loose aggregation. The loose aggregation is located at the outermost surface which appears heterogeneously in light gray and consists of a silicon rich oxide mixture [4]. The silicon is assumed to be a contaminant from the dissolution of the glass ampoule by the alkaline solution. Unless the Si precipitate becomes dense, the loose aggregation is considered to have no effect on corrosion resistance.

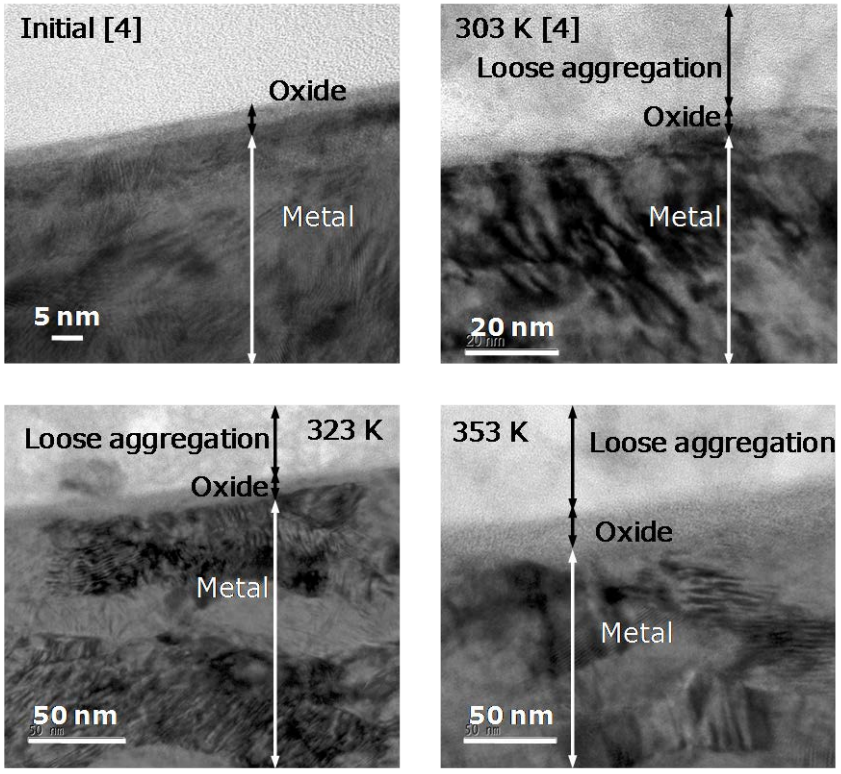

Fig. 5. TEM observation of the surface oxide after 24 months corrosion at different temperatures.

The second surface located on the metallic phase is an oxide that is generally referred to as passive film. Table II summarizes the oxide thickness data obtained by TEM together with the magnetite thickness (x) calculated using Eq. 4. At 303 K, the increase in the thickness of this oxide portion from the initial value of 3 nm is negligible. At 323 K, the oxide thickness slightly increases with corrosion time. The rise in temperature also affects oxide growth. The magnetite thickness is slightly thicker than that seen in TEM. It is possible that a part of magnetite is dissolved in the solution. Fig. 6 shows the elemental composition, by EDX, of the oxide portion after 24 months corrosion at 353 K together with the electron diffraction pattern. Similar data have been obtained at 303 K [4] and 323 K. The oxide consists of iron and chrome, and is amorphous. However, it is not clear whether there is any formation of magnetite or chrome base passive oxide.

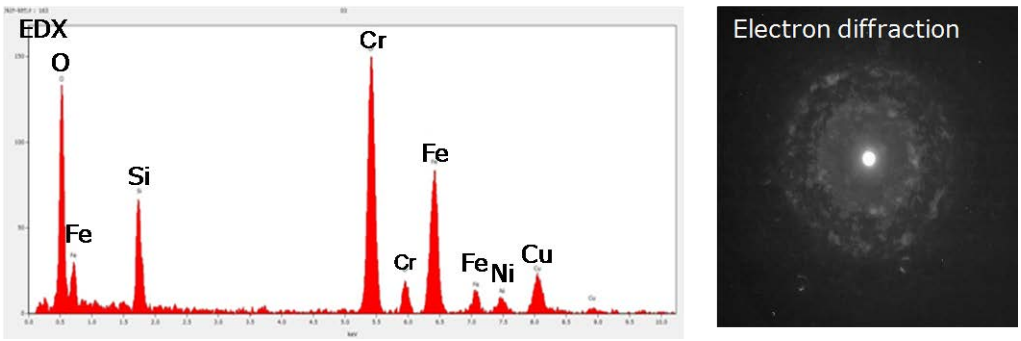

Fig. 6. EDX spectrum (left) and electron diffraction (right) of oxide after 24 months corrosion at 353 K.

Fig. 7 shows the elemental composition and depth distribution of the oxide as measured by XPS. The initial oxide thickness is less than 10 nm, roughly corresponding to the TEM observation (Fig. 5) [4]. The slight discrepancy of the oxide thickness results between the TEM and XPS methods may be attributable to the influence of surface roughness and sputter rate correction. After corrosion occurs, an Si-rich region appears which is approximately 30 nm to 50 nm at 303 K

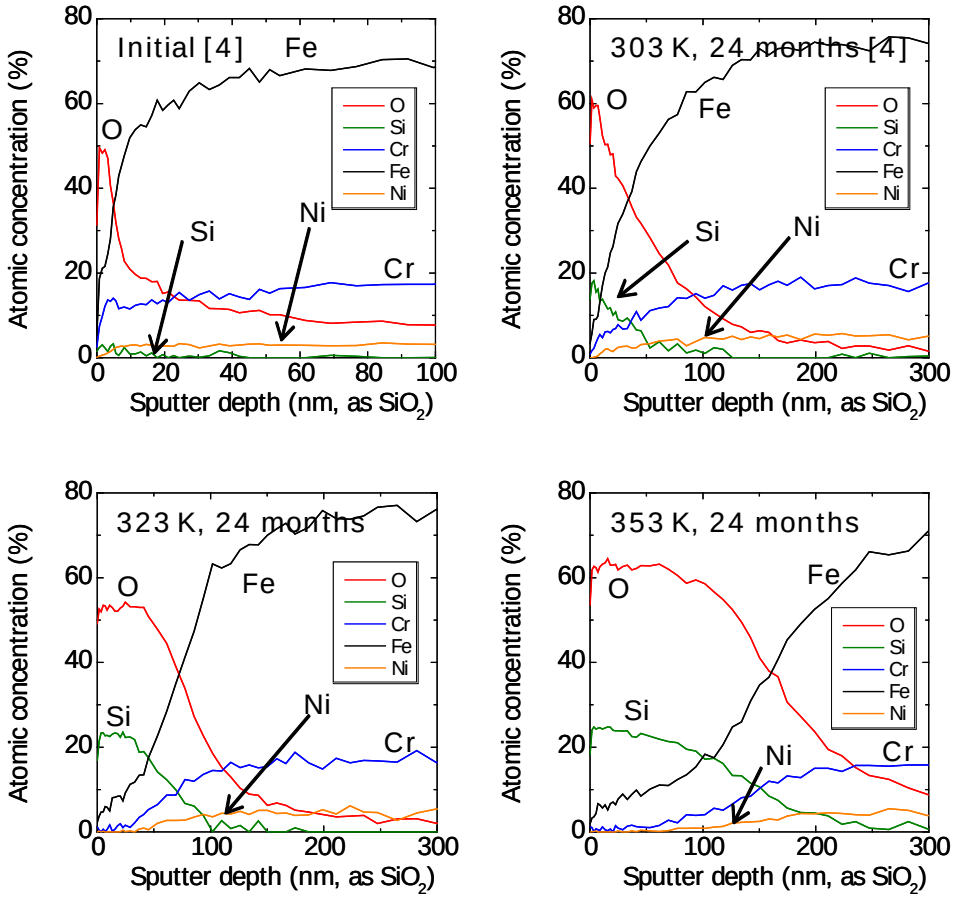

Fig. 7. Depth profiles of elements by XPS measurement before and after 24 months of corrosion at different temperatures. Data for initial conditions and 303 K are obtained from published study [4].

[4]. This region corresponds to the loose aggregation shown in Fig. 5 and expands with temperature. Because the oxide composition is not clearly determined by XPS in the profile, it is difficult at present to identify the characteristics and role of the oxide film that was formed under both high temperatures and in situ temperature. Detailed analysis for the characterization of oxide is expected to be subject for further study.

Table II. Summary of stainless steel corrosion data.

Temp. (K)	Test time (days)	A_{gas} ($mol \cdot m^{-2}$)	Rc ($\mu m \cdot a^{-1}$)	x (cm)	k_p ($cm^2 \cdot s^{-1}$)	Oxide thickness by TEM (nm)
303	90	1.29×10^{-4}	1.40×10^{-3}	7.20×10^{-8}		
	90	1.69×10^{-4}	1.83×10^{-3}	9.43×10^{-8}		
	180	2.48×10^{-4}	1.34×10^{-3}	1.38×10^{-7}	8.77×10^{-23}	
	180	2.30×10^{-4}	1.24×10^{-3}	1.28×10^{-7}	$\pm 7.2 \times 10^{-24}$	
	360	3.73×10^{-4}	1.01×10^{-3}	2.08×10^{-7}		
	360	3.08×10^{-4}	8.31×10^{-4}	1.72×10^{-7}		
	720	4.68×10^{-4}	6.32×10^{-4}	2.61×10^{-7}		2 - 4
	720	6.89×10^{-4}	9.29×10^{-4}	3.83×10^{-7}		
323	90	3.54×10^{-4}	3.82×10^{-3}	1.97×10^{-7}		
	90	4.31×10^{-4}	4.66×10^{-3}	2.40×10^{-7}		2 - 4
	180	7.47×10^{-4}	4.03×10^{-3}	4.16×10^{-7}	9.15×10^{-22}	
	180	6.38×10^{-4}	3.44×10^{-3}	3.55×10^{-7}	$\pm 1.0 \times 10^{-22}$	
	360	1.02×10^{-3}	2.76×10^{-3}	5.70×10^{-7}		4 - 7
	360	1.24×10^{-3}	3.35×10^{-3}	6.92×10^{-7}		
	720	1.83×10^{-3}	2.47×10^{-3}	1.02×10^{-6}		5 - 10
	720	2.10×10^{-3}	2.84×10^{-3}	1.17×10^{-6}		
353	90	1.82×10^{-3}	1.96×10^{-2}	1.01×10^{-6}		
	90	1.85×10^{-3}	2.00×10^{-2}	1.03×10^{-6}		
	180	2.52×10^{-3}	1.36×10^{-2}	1.40×10^{-6}	9.32×10^{-21}	
	180	2.13×10^{-3}	1.15×10^{-2}	1.19×10^{-6}	$\pm 5.8 \times 10^{-22}$	
	360	3.31×10^{-3}	8.94×10^{-3}	1.84×10^{-6}		
	360	3.75×10^{-3}	1.01×10^{-2}	2.09×10^{-6}		
	720	4.87×10^{-3}	6.57×10^{-3}	2.71×10^{-6}		7 - 14
	720	6.42×10^{-3}	8.67×10^{-3}	3.58×10^{-6}		

CONCLUSION

The effect of temperature on corrosion behavior of 18Cr−8Ni austenitic stainless steel in a deoxygenated NaOH solution was investigated in the range of 303 K to 353 K over 2 years. The corrosion rates decreased with time but increased with rising temperature, and had average values after 24 months of 7.80×10^{-4} at 303 K, 2.65×10^{-3} at 323K, and 7.62×10^{-3} $\mu m \cdot a^{-1}$ at 353 K. All values are lower than the 2.0×10^{-2} $\mu m \cdot a^{-1}$ that is used as the assumed rate for corrosion of stainless steel under safety assessment in Japan. The corrosion kinetics follows a parabolic rate law. The activation energy evaluated by the Arrhenius relationship was found to be 82.5 ± 6.2 kJ/mol, which corresponds to the energy for high temperatures down to 423 K. This indicates that the corrosion processes at high and in situ temperature are almost the same and that they are under diffusion control. This result, however, has not yet been thoroughly explained with respect to oxide film characteristics. From the perspective of long-term safety, it is notable that the high temperature behavior, when regarded as an acceleration test against the extremely

slow corrosion at in situ temperatures, will facilitate good estimation for the eventual state of stainless steel waste after disposal in geological media.

REFERENCES

1. Federation of Electric Power Companies (FEPC) and Japan Atomic Energy Agency (JAEA), Second Progress Report on Research and Development for TRU Waste Disposal in Japan (2007).
2. T. Sakuragi, H. Tanabe, E. Hirose, A. Sakashita and T. Nishimura, Estimation of Carbon 14 Inventory in Hull and End-Piece Wastes from Japanese Commercial Reprocessing Operation, Proceedings of the ASME 2013 15th International Conference on Environmental Remediation and Radioactive Waste Management, ICEM2013, September 8-13, 2013, Brussels, Belgium (2013).
3. International Atomic Energy Agency, Durability of Spent Nuclear Fuels and Facility Components in Wet Strage, IAEA-TECDOC-1012, Vienna (1998).
4. T. Sakuragi, Y. Yoshida, O. Kato and T. Tateishi, Study of Stainless Steel Corrosion by Hydrogen Measurement under Deoxygenated, Low-temperature and Basic Repository Conditions, Progress in Nuclear Energy **87** (2016), 26-31.
5. J. Robertson, The Mechanism of High Temperature Aqueous Corrosion of Stainless Steels, Corrosion Science **32** (1991), 443-465.
6. T. Maekawa, M. Kagawa and N. Nakajima, Corrosion Behavior of Stainless Steel in High-temperature Water and Superheated Steam, Trans. JIM **9** (1968) 130-136.
7. M. Mihara, T. Nishimura, R. Wada and A. Honda, Estimation on Gas Generation and Corrosion Rates of Carbon Steel, Stainless Steel and Zircaloy in Alkaline Solutions under Low Oxygen Condition, Japan Nuclear Cycle Development Institute Engineering Reports No. 15, 2002 (2002) (in Japanese)
8. A. Honda, T Nishimura, R. Wada and M. Tanabe, Long Term Testing System, Testing Container and Measurement Container, Japan Patent 2912365 (1999).
9. T. Sakuragi, H. Miyakawa, T. Nishimura and T. Tateishi, Corrosion Rates of Zircaloy 4 by Hydrogen Measurement under High pH, Low Oxygen and Low Temperature Conditions, Mater. Res. Soc. Symp. Proc. **1475** (2012), 311-316.

ACKNOWLEDMENT

This research is a part of the “Research and development of processing and disposal technique for TRU waste (FY2014)” program funded by Agency for Natural Resources and Energy in Ministry of Economy, Trade and Industry of Japan.